약학석사 학위논문

Natural polysaccharide complexed with RNA nanoadjuvant for cancer immunotherapy

천연 다당류와 RNA 나노 어쥬번트 복합체를 이용한 면역항암치료 연구

2020 년 2 월

서울대학교 약학대학원

약학과 물리약학 전공

최 진 주

Natural polysaccharide complexed with RNA nanoadjuvant for cancer immunotherapy

천연 다당류와 RNA 나노 어쥬번트 복합체를 이용한 면역항암치료 연구

지도교수 오 유 경

이 논문을 약학석사 학위논문으로 제출함

2020 년 1 월

서울대학교 약학대학원

약학과 물리약학 전공

최 진 주

최진주의 석사 학위논문을 인준함

2020 년 1 월

위 원 장 이 봉 진 (인)

부위원장 변 영 로 (인)

위 원 오 유 경 (인)

Abstract

Natural polysaccharide complexed with RNA nanoadjuvant for cancer immunotherapy

Jin Joo Choi

Physical Pharmacy, Department of Pharmacy

The Graduate School

Seoul National University

Recently, nucleic acid adjuvants have emerged as a promising application in cancer vaccine for inducing tumor suppressing immune cells. In this study, we screened for the optimal complexation ratio and molecular weight of chitosan (CTS) as a delivery system for toll-like receptor 3- recognizing RNA adjuvant (RA). Anionic RA formed a nanocomplex with cationic CTS by electrostatic interaction, possessing positive zeta potentials. CTS protected RA from degradation by serum or RNase. RA/CTS formed with various molecular weights of CTS showed no cytotoxicity in bone marrow derived dendritic cells

(DC). High molecular weight of CTS (340K) induced much higher maturation in splenic DC than other RA/CTS with lower molecular weights. RA/CTS (340K) significantly improved DC maturation effect in vivo as compared with RA only group. Naive mice were inoculated with ovalbumin (OVA)-expressing B16F10 tumor after receiving the physical mixture of RA/CTS and OVA thrice. Tumorigenesis of the mice pretreated with RA/CTS was observed to be delayed the most compared to other groups. Mechanistically, the RA/CTS-treated mice showed the highest OVA antigen-specific humoral and cellular immune response after tumor challenge. Moreover, CD4 helper T cell and CD8 T cell were most frequently infiltrated into the tumor tissue of RA/CTS treated mice. When re-challenged with tumor after 69 days from the first inoculation, RA/CTS-pretreated mice still exerted anti-tumor adaptive immune response, resulting in 100% survival rate for 110 days. Our results suggest that RA/CTS nanocomplex can serve as an effective nanoadjuvant in the design of tumor vaccines and cancer immunotherapy.

Keywords : Nucleic acid adjuvant, chitosan, molecular weight screening, cancer vaccine, immunotherapy
Student Number : 2017-27650

Table of Contents

List of Figures

1. Introduction

Cancer vaccines have been extensively studied to generate an active anti-tumor immune system to fight against tumor [1]. A successful cancer vaccine is required to elicit a robust and long-lasting immune response against tumor antigens. Key formulation of cancer vaccines includes an immunostimulatory agent called vaccine adjuvants to yield stronger immune response along with tumor antigen. Alum derivatives are most well-known vaccine adjuvant for their ability to provoke immunity and boost the humoral immune response [2]. However, they fail to generate an effective cellular immune response, which is crucial for anti-tumor activity [2-3].

Nucleic acid-based adjuvants have emerged as a new class of adjuvants for cancer vaccines in term of high biocompatibility and potency [4-7]. The CpG or poly I:C are representative nucleic acid adjuvants which are able to generate cytotoxic T lymphocytes resulting in toxicity towards the tumor cells [4-6]. Although proving the potential activity in term of boosting anti-tumor immune response, clinical trials of nucleic acid adjuvants, in cancer treatment still face the unimpressive outcomes [7].

There are some limitations of nucleic acid adjuvant in clinical use [7-9]. First, the target molecules of these nucleic acid adjuvant located intracellularly require efficient penetration of adjuvant into the cell to reach the targets [8]. Since nucleic acid adjuvant is negatively charged in nature, permeation through negatively charged cell membrane is difficult. Secondly, nucleic

acid adjuvants are extremely unstable under presence of nucleases such as DNase or RNase, found ubiquitously in body fluids. Quick degradation shortly after administration limits the efficacy of these adjuvants [7,9]. Therefore, the delivery systems that can protect these nucleic acid adjuvants from enzyme degradation and further enhance uptake by dendritic cell, is required.

Chitosan (CTS), a naturally derived polymer composed of linear polysaccharide, has been used intensively in biomedical engineering and drug delivery due to the nature of biodegradability and excellent biocompatibility [10]. Various studies have adopted CTS as a carrier for nucleic acid-based gene materials owing to the rich presence of versatile amine groups in CTS backbone. The protonation of these amines at acidic pH induces CTS to be positively charged, and thus to easily condense with gene material to form nanocomplexes. By complexation, CTS is able to protect nucleic acid from enzyme-mediated degradation and improve the internalization of nucleic acid cargo into the cell. Although CTS can be a potential carrier for nucleic acid adjuvant delivery, according to previous studies, careful screening is required for suitable molecular weight of polymer dependent on characteristics of nucleic acid materials [11-12].

Herein, we tested CTS at various molecular weight range as a delivery system for nucleic acid adjuvant. In this study, we adopted poly I:C-derived double stranded RNA adjuvant (RA) and ovalbumin (OVA) as a model nucleic acid adjuvant and an antigen, respectively. Negatively charged RA was complexed with

cationic CTS polymer forming nanocomplexes (RA/CTS) and were treated in vivo to confirm anti-tumor adaptive immune response as illustrated in Figure 1-2.

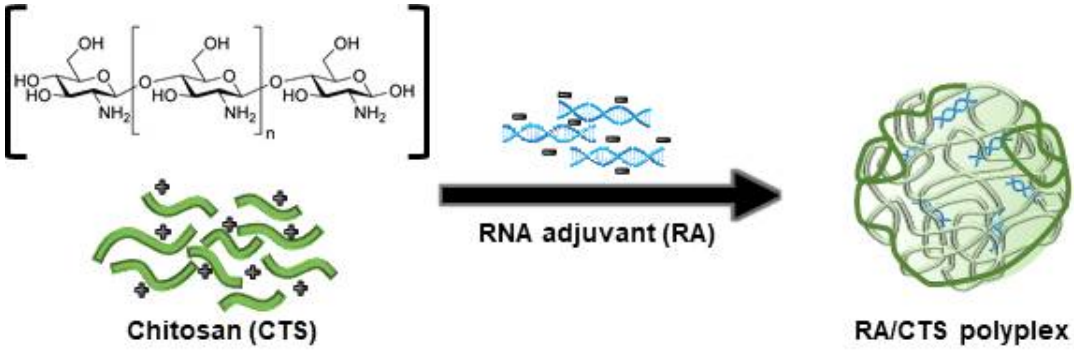

Figure 1. Formation of RA/CTS nanocomplex.

RA was complexed with CTS to form RA/CTS nanocomplex by electrostatic interactions.

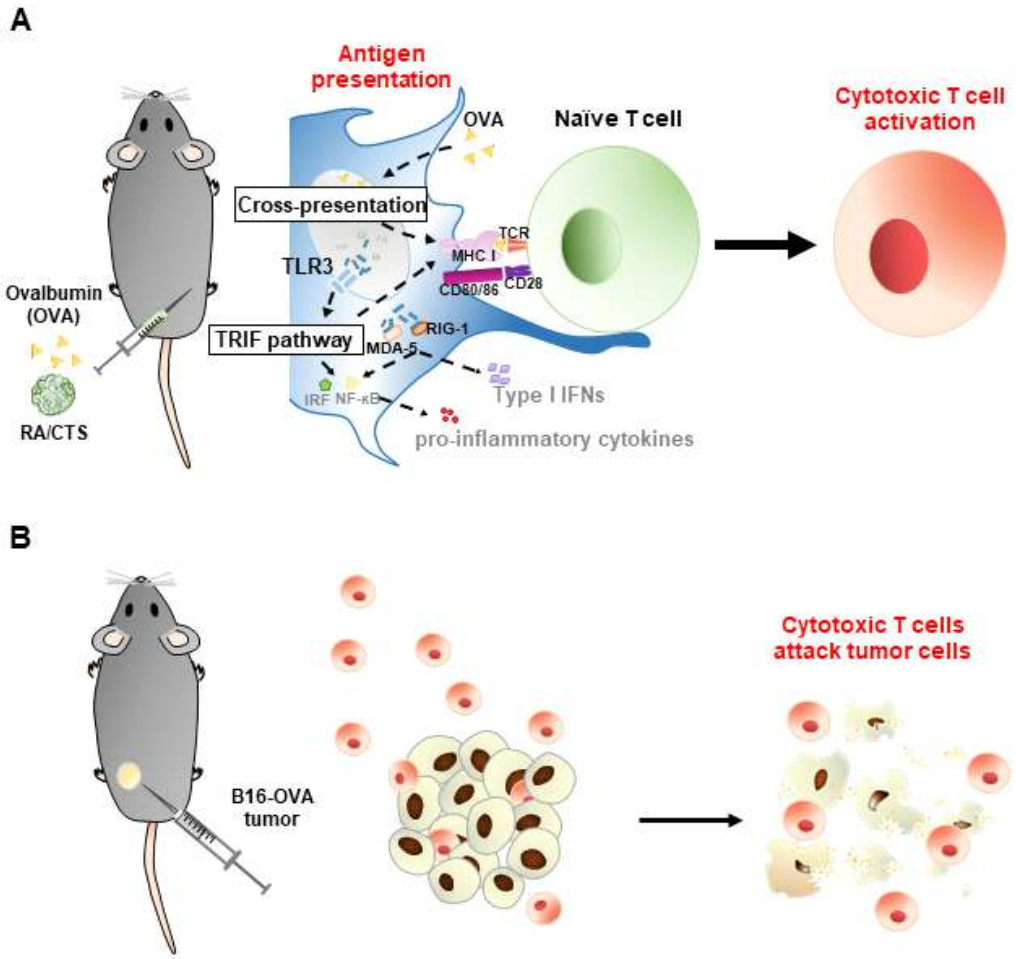

Figure 2. Schematic illustration of RA/CTS nanocomplex as immune-modulating vaccine for cancer therapy.

(A) Subcutaneous injection of RA/CTS with OVA antigen activates dendritic cells for migration to nearby lymph nodes for subsequent antigen presentation. When presented with MHCI-OVA (antigen) complex and co-stimulatory signals, naive T cells are consequently differentiated into OVA-specific cytotoxic T cells. (B) These cytotoxic T cells are capable of killing tumor cells expressing OVA, thus functioning as a cancer vaccine.

2. Materials and Methods

2.1 Preparation of RA-complexed CTS (RA/CTS) nanocomplexes

RA/CTS nanocomplexes were formed by electrostatic interactions of cationic CTS low (120kDa (K)), medium (250K), and high (340K) average molecular weights (Sigma-Aldrich, St. Louis, MO, USA) and anionic RA (NA Vaccine Institute, Seoul, South Korea). Briefly, 10 mg of CTS was dissolved in 1% acetic acid 400 μg/mL) and stirred overnight at 50 ^{0}C. The CTS solution was then filtered through 0.45 μm polycarbonate membrane filter (Millipore Corp., Billerica, MA, USA). The resulting CTS solution was titrated to pH 6.5 before complexation with RA, or stored at 4 ^{0}C until use. To form nanocomplex, CTS was physically mixed with RA (1 mg/mL in TDW) at 1:10 (w/w, RA:CTS) ratio. The mixture was allowed to sit for 15 minutes before use in experiments.

2.2 Characterization of RA/CTS nanocomplexes

Nanocomplexes were characterized by morphology, size, and zeta potential. Morphologies of RA/CTS nanocomplexes were examined with transmission electron microscopy (TEM; Talos L120C, Thermo Fisher Scientific, Waltham, MA, USA). Size of nanocomplexes was measured using dynamic light scattering technique while zeta potential was measured by laser Doppler microelectrophoresis using an ELSZ-1000 instrument (Otsuka Electronics Co. Ltd., Osaka, Japan).

2.3 Complexation and stability of RA/CTS nanocomplexes

Complexation and stability of RA/CTS were confirmed by gel retardation assay. The nanocomplexes were prepared by adding CTS to RA (200 ng) with various RA:CTS ratio (1:0, 1:1, 1:2, 1:5, 1:10, 1:20 w/w), and incubated at room temperature for 15 minutes. Then, the samples were electrophoresed in 1% (w/v) agarose gel and visualized under Gel Doc XR+ Imaging System (Bio-Rad, Hercules, CA, USA). For stability against enzymatic digestion, RA (200 ng) and CTS were mixed at a w/w ratio of 1:10 and incubated at room temperature for 15 minutes. After adding RNase A (80 μg/mL; Qiagen, Hilden, Germany), or fetal bovine serum (FBS; GenDEPOT, Barker, TX, USA) at a final concentration of 50% (v/v), the samples were incubated at room temperature for 15 minutes. For staining, 10X Safe-Pinky DNA Gel Staining Solution (GenDEPOT) was used. The stained samples were then electrophoresed in 1% (w/v) agarose gel for 15 minutes. Naked RA was treated under identical conditions as controls.

2.4 Isolation of bone marrow-derived dendritic cells (BMDC)

BMDCs were isolated and differentiated from monocytes as previously described, with minor modifications [13]. Six-week-old female C57BL/6 mice were purchased from Raon Bio (Yongin, South Korea). All animal experiments followed

Guidelines for the Care and Use of Laboratory Animals of the Institute of Laboratory Animal Resources (Approved animal experimental protocol number, SNU-180914-4). Briefly, femurs and tibiae from C57BL/6 mice were isolated and flushed inside with complete RPMI media to collect bone marrow. Red blood cells were lysed to obtain monocyte pellets which were suspended and cultured in Iscove's modified Dulbecco's medium (IMDM) supplemented with 10% FBS (GenDEPOT), 100 units/mL penicillin, 100 mg/mL streptomycin (Gibco, Carlsbad, CA, USA), 20 ng/mL recombinant mouse GM-CSF, 20 ng/mL recombinant mouse IL-4 (GenScript, Piscataway, NJ, USA), and 50 μM β-mercaptoethanol (Sigma-Aldrich). The medium was changed every 3 days and the cells were harvested for experiment on day 7.

2.5 Intracellular uptake pathway test

DC uptake pathways of RA/CTS nanocomplexes were explored using various chemicals inhibiting specific pathways of cellular entry. Genistein (200 μM; Sigma-Aldrich) inhibiting caveolae-mediated pathway [14], chlorpromazine (10 μM; Sigma-Aldrich) and sucrose (450 mM; Affymetrix, Cleveland, OH, USA) inhibiting clathrin-mediated pathway [15], and amiloride (1 mM; Sigma-Aldrich) inhibiting macropinocytosis [16] were used. Block-iT^{TM} (BiT), a fluorescein-labelled dsRNA oligomer (Invitrogen, Carlsbad, CA, USA) complexed with CTS 340K (BiT/CTS) were used at a weight ratio of 1:20 to visualize the intracellular delivery. Briefly, BMDCs were seeded in 24-well plates, and treated with chemical inhibitors in RPMI

media for 30 min prior to sample treatment. The BiT/CTS was treated to the BMDCs with a BiT concentration of 2 μg/mL. After 4h treatment of samples, the cells were washed with 2% FBS in PBS and analyzed using BD FACSCalibur flow cytometer (BD Bioscience, San Jose, CA, USA) and CellQuest Pro software. FlowJo software v10.0.7 (BD Bioscience) was also used for analysis.

2.6 *In vitro* cell viability assay

In vitro cell viability was assessed by live cell staining (Biomax, Seoul, South Korea) and MTT (3-(4,5-dimethylthizol-2-yl)-2, 5-diphenyltetrazolium bromide) assay (Sigma-Aldrich). BMDCs were seeded in 48-well plates and 96-well plates with approximately 95% confluence for live cell imaging and MTT assay, respectively. After treating with various molecular weights of CTS (100 μg/mL) and RA/CTS (RA 10 μg/mL, CTS 100 μg/mL) formulations for 24 hours, the cells were stained with calcein (2 μM) for 15 minutes. Live cells were visualized by a fluorescence microscopy (Leica DM IL, Wetzlar, Germany). For MTT assay, after treatment with formulations for 24 hours, the cells were incubated with 250 μg/mL MTT (stock concentration 2.5 mg/mL) for 2 hours at 37°C. After solubilization of formazans with DMSO, the absorbance of each well was measured at 570 nm using a SpectraMax M5 plate reader (Molecular Devices, Sunnyvale, CA, USA).

2.7 *In vitro* assessment of RA/CTS-mediated DC activation

DC activation was evaluated by the expression of specific surface markers on splenic dendritic cells by flow cytometry. Splenocytes were isolated from naive C57BL/6 mice. These cells were seeded in 24-well plates and were treated with RA/CTS formulations for 24 hours. Then, the cells were harvested and stained with FITC-conjugated anti-mouse CD11c antibody and APC-conjugated anti-mouse CD80 or CD86 (BioLegend, San Diego, CA, USA) antibodies for 1 hour. After washing with 2% FBS in PBS, the expression of these surface markers were analyzed using a BD FACSCalibur flow cytometer (BD Bioscience) and CellQuest Pro software. The data were also analyzed using FlowJo software v10.0.7 (BD Bioscience).

2.8 *In vivo* assessment of RA/CTS-mediated DC activation

DC activation was evaluated by the expression of specific surface markers on splenocytes isolated from C57BL/6 mice. These mice were injected with CTS HMW(100 μg) intraperitoneally and splenocytes were isolated after 24 hours. Isolated splenocytes were harvested and stained with FITC-conjugated anti-mouse CD11c antibody and APC-conjugated anti-mouse CD80 and CD86 (BioLegend). The expression of these surface markers on DCs were analyzed by gating CD11c+population.

2.9 *In vivo* study of anticancer efficacy

In vivo anticancer efficacy was tested after immunizing naive C57BL/6 mice with CTS and RA/CTS HMW formulations (RA 10 μg, CTS 100 μg) and subsequently challenging with B16F10 tumor cell line transfected with OVA plasmid (B16-OVA). B16-OVA was cultured in DMEM medium (Gibco) supplemented with 10% FBS (Gibco), 100 units/mL penicillin, 100 mg/mL streptomycin (Gibco). RA/CTS (10: 100 μg/mouse) and OVA (100 μg/mouse; Sigma-Aldrich) were injected subcutaneously in the right flank three times at 4-day intervals (day -13, -9, -5). On day 0, B16-OVA cells (3×10^5) were also injected subcutaneously. Tumors were measured with calipers, calculating volumes with the equation $a \times b^2 \times 0.5$. Here, a is the longest and b is the shortest dimension [13]. To confirm long-term tumor protection from vaccination, cured mice were re-challenged with same tumor cells at a different site. On day 69 after first tumor inoculation, mice were re-challenged with 2×10^6 B16-OVA cells subcutaneously. Tumor growth from re-challenge was monitored for 27days. Naive mice without vaccination were included as a control group.

2.10 Ex vivo analysis of antigen-specific immune T cell response

To evaluate in vivo T cell priming by vaccination, number of IFN-γ secreting cells in splenocytes were detected via ELISPOT assay (BD Bioscience). C57BL/6 mice were immunized with RA/CTS HMW and OVA antigen (100 μg) every 4 days for 3 times. Five days after the last immunization, mice were

challenged with B16-OVA tumor. And 2 days after the tumor challenge, splenocytes were isolated. These cells were seeded onto an IFN-γ ELISPOT plate (2 x 10^7 cells/well) and re-stimulated with class I (Kb)-restricted peptide epitope of OVA, OVA(257-264)(5 μg/mL; GenScript) for 24 hours. Then, following the manufacturer's instructions, IFN-γ secreting cells indicated by spot development were detected and were counted manually using stereomicroscope (SZ51; Olympus, Tokyo, Japan).

2.11 Measurement of OVA-specific IgG antibody titer

An enzyme-linked immunosorbent assay (ELISA; Invitrogen) was conducted to evaluate immunoglobulin (IgG) isotypes of anti-OVA antibodies in serum of immunized mice. Serum was collected 6 and 10 days after tumor challenge. Briefly, 96-well ELISA plates were coated with 100 μg/mL OVA (Sigma-Aldrich) in PBS overnight at 4 ^{0}C. After washing with 0.05% Tween20/PBS (PBST), plates were blocked for 1 hour in 10% FBS in PBS at 37^{0}C. After thorough washing with PBST, diluted serum samples were added to each well and incubated with gentle shaking for 2 hours. Then, the plates were washed again with PBST and incubated with horseradish peroxidase (HRP)-conjugated rat anti-mouse IgG (1 μg/mL in 10% FBS) for 2 hours with gentle shaking. Finally, the plates were washed and 3,3′,5,5′-tetramethylbenzidine (TMB) substrate was added. After 10 minutes, the reaction was stopped with sulfuric

acid (0.16M). Then, the absorbance was detected at 450 nm with SpectraMax M5 plate reader (Molecular Devices).

2.12 T cell infiltration assay

On day 27 after tumor challenge, tumor-infiltrating T cells were analyzed by flow cytometry. First, tumor tissues were excised and digested in collagenase (1 mg/mL in RPMI; Sigma-Aldrich) for 2 hours at 37 ^{0}C under gentle stirring. Red blood cells were lysed and the resulting tumor cell suspension was passed through a 40 μm strainer. Then, the cells were stained with fluorescent antibodies: APC-conjugated anti-mouse CD3 antibody (BioLegend), PE-conjugated anti-mouse CD4 antibody (BioLegend), PerCP/cyanine5.5-conjugated anti-mouse CD8a antibody (BioLegend). The percentage of CD3+CD4+and CD3+CD8+ cells were analyzed using a BD FACSCalibur flowcytometer, CellQuest Pro and FlowJo software v10.0.7 (BD Bioscience).

2.13 Measurement of effector memory T cell populations

Seven days after tumor re-challenge with B16-OVA tumor (2 x 10^{6} cells/mouse), inguinal lymph nodes closest to the tumor were isolated for effector memory T cell analysis. Strainers (40 μm) were used to dissociate tissues into single cells. Red blood cells were lysed and the resulting cell populations were stained with fluorescent antibodies: FITC-conjugated anti-mouse CD3 antibody (BioLegend), PerCP/cyanine5.5-conjugated anti-mouse CD8a (BioLegend), PE-conjugated anti-mouse CD62L

(BioLegend), and APC-conjugated anti-mouse CD44 (BioLegend). The percentage of effector memory T cells ($CD3^+CD8^+CD44^{high}CD62^{low}$) was analyzed using a BD FACSCalibur flow cytometer (BD Bioscience), CellQuest Pro and FlowJo software v10.0.7.

2.14 Statistics

Data were analyzed by one-way analysis of variance (ANOVA), followed by Student—Newman—Keuls post hoc test for statistical evaluation of experimental data. SigmaStat software (version 12.0; Systat Software, Richmond, CA, USA) was used and *P* values less than 0.05 were considered statistically significant.

3. Results

3.1 Characterization of RA/CTS

The physicochemical properties of RA/CTS were demonstrated by morphology, complexation, size, and zeta potentials. To confirm optimal complexation ratio between RA and CTS, gel retardation was conducted (Figure 3). Since no residual RA was observed at RA/CTS at a weight ratio of 1:10, all of the added RA appear bound to CTS. Size distribution (Figure 4A) and average particle size (Figure 4B) was determined by dynamic light scattering (DLS). The mean size of RA/CTS LMW was 362.0 ± 43.6 nm, while RA/CTS MMW and RA/CTS HMW were 355.3 ± 31.9 nm and 415.6 ± 19.6 nm, respectively (Figure 4B). Similar to DLS results, the addition of various MW CTS (1:10, w/w) did not show significant differences between zeta potential values (Figure 5). Morphology of the RA/CTS was examined via TEM imaging (Figure 6).

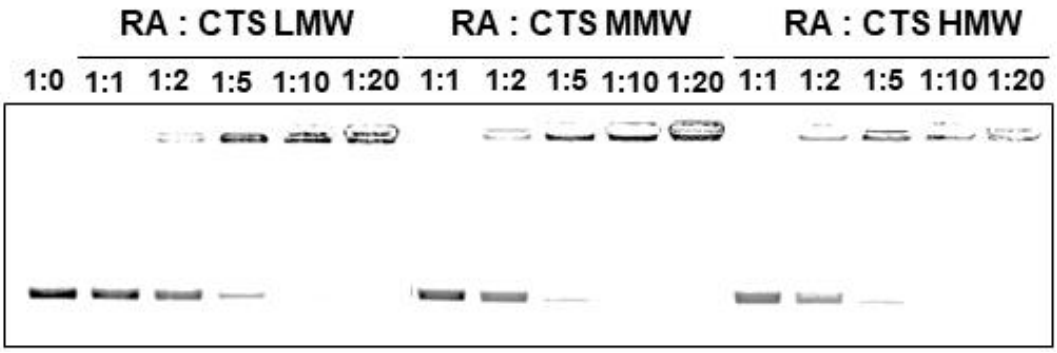

Figure 3. Gel retardation of RA/CTS nanocomplex.

Complexation between RA and CTS were tested at various weight ratios by gel retardation assay.

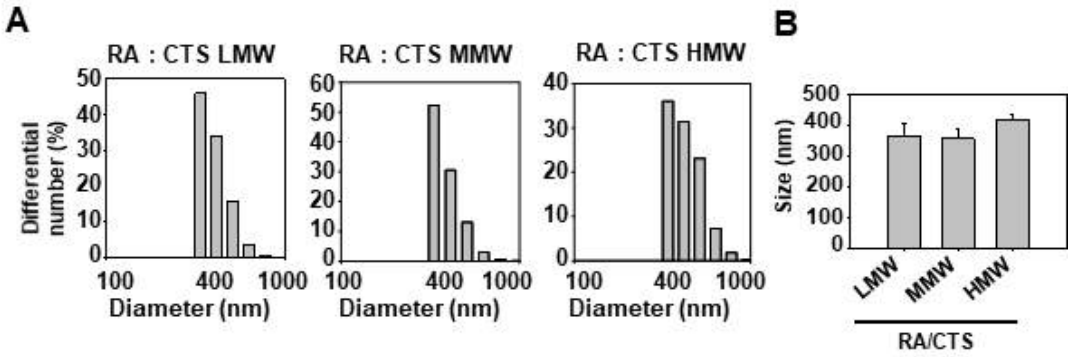

Figure 4. Size of RA/CTS nanocomplex.

Size distribution (A) and average size (B) of RA/CTS nanocomplex were measured by dynamic light scattering.

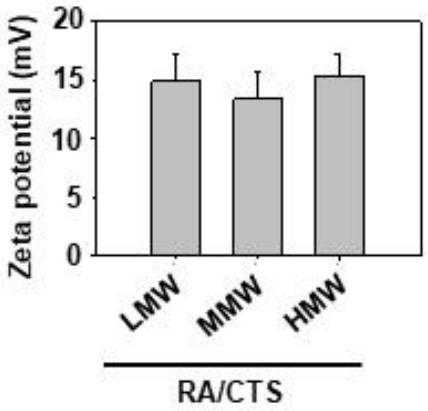

Figure 5. Zeta potential of RA/CTS nanocomplex.

Zeta potentials were obtained from RA/CTS with low, medium, or high molecular weights.

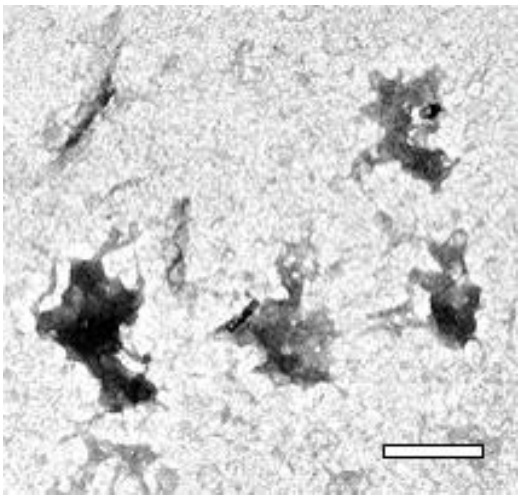

Figure 6. TEM imaging of RA/CTS nanocomplex.
Morphology of RA/CTS HMW (1:10, w/w) was observed. Scale bar, 500nm.

3.2 Stability of RA/CTS

Complexation with CTS provided RA stability in biologically relevant conditions. Stability of naked RA and RA/CTS HMW was examined by incubating with serum and enzyme. After incubation with FBS, naked RA degraded as shown by the broad band (Figure 7A). In contrast, complexation with CTS protected RA from degradation. When incubated with RNase A, RA/CTS was also resistant to degradation while naked RA was fully degraded (Figure 7B).

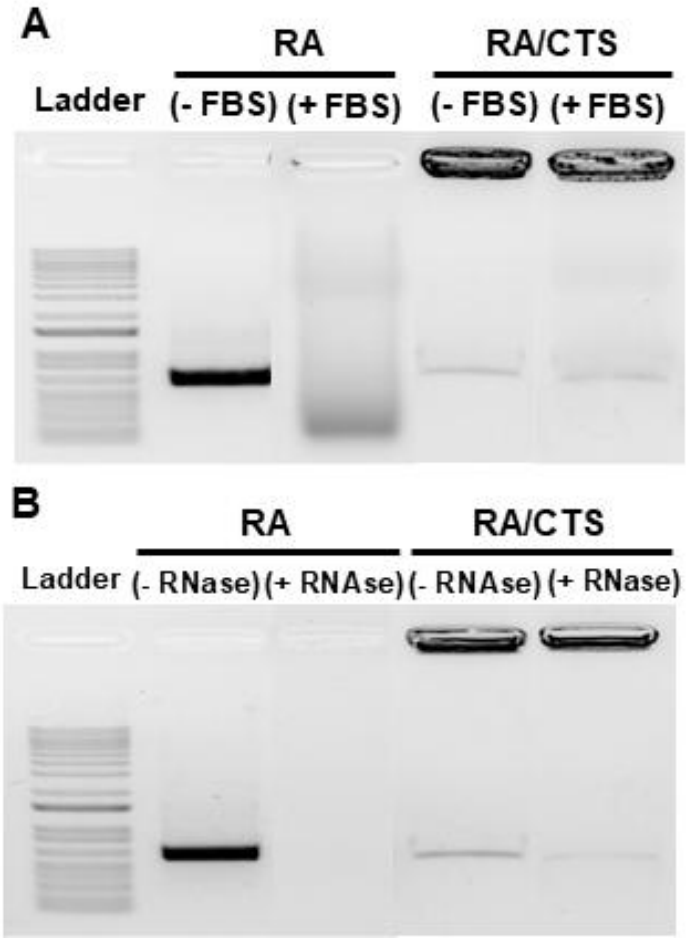

Figure 7. Stability of RA/CTS nanocomplex.

Stability of RA in free form or CTS-complexed form was analyzed against enzymatic degradation. After incubation with FBS (A) or RNase (B) for 15 minutes, naked RA or RA/CTS was electrophoresed on agarose gel.

3.3 Intracellular uptake pathway of RA/CTS

The intracellular pathways in which RA/CTS nanoomplexes would be taken up by BMDCs were examined using endocytic inhibitors genistein (caveolae-mediated pathway), chlorpromazine (clathrine-mediated pathway), sucrose (clathrine-mediated pathway), and amiloride (macropinocytosis). RA was substituted with fluorescent RNA (block-iT) for flow cytometry. While chlorpromazine, sucrose, and amiloride significantly inhibit the cellular uptake of block-iT/CTS (B-iT/CTS), genistein seems to have no effect on the intracelllular uptake (Figure 8).

3.4 Cytotoxicity of RA/CTS

Cell viability of BMDC was evaluated after treatment of RA/CTS formed with various molecular weight CTS. As shown in Figure 9A, cytotoxicity on BMDC were negligible when compared with untreated or naked RA-treated BMDC. Cell viabilities of BMDC treated with various CTS complexed RA were all above 80% (Figure 9B).

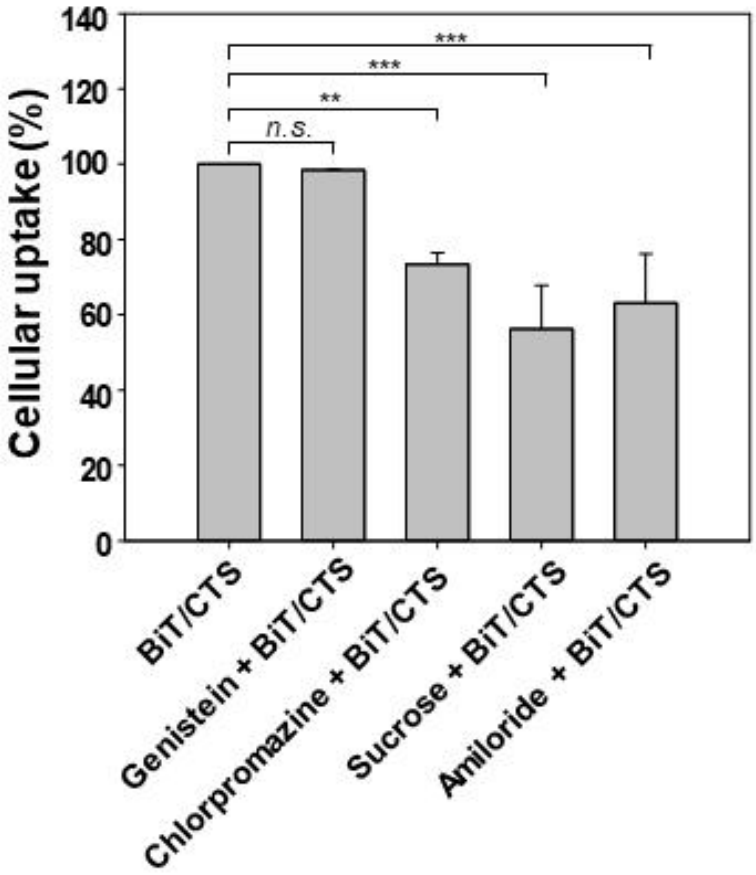

Figure 8. Effects of endocytic inhibitors on the uptake of block-iT/CTS (BiT/CTS) nanocomplexes by BMDCs.

After pre-treatment of genistein (200 μM), chlorpromazine (10 μM), sucrose (450mM), amiloride (1mM) in media for 30 minutes, BiT/CTS nanocomplexes were then added for 4 hours. Then the cells were washed for flow cytometry. Data shown as mean ± SEM, n = 3.

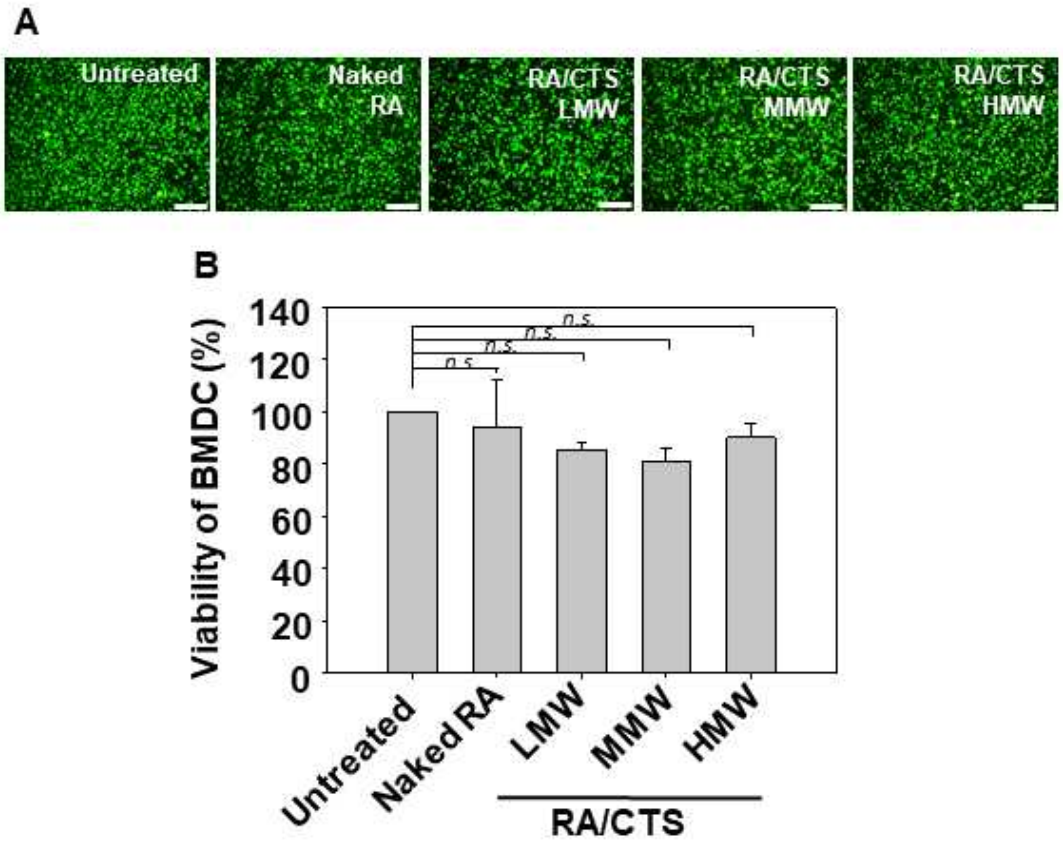

Figure 9. Viability of BMDC treated with RA/CTS.

Viability of BMDC was shown using live cell imaging (A) and MTT assay (B) after 24 hour incubation with naked RA and RA complexed with various molecular weight CTS.

3.5 *In vitro* DC maturation effect of RA/CTS

To compare DC maturation ability of RA/CTS nanocomplexes between different molecular weights of CTS, surface expression of CD80 was analyzed (Figure 10A, 10B). RA/CTS HMW showed the highest maturation effect among other MW formulations, (Figure 10B). Moreover, the percentage of CD11c+CD80+ cells of RA/CTS HMW was 14.4 and 72-fold higher than untreated and naked RA-treated cells, respectively (Figure 10B).

3.6 Immune boosting effect of RA/CTS

To compare molecular weight dependence on immune response, humoral immune response was examined after vaccination with RA/CTS nanocomplexes of various molecular weight CTS, followed by tumor challenge (Figure 11A). Serum anti-OVA IgG antibody levels were used as indicator of humoral immune response. Out of the molecular weights tested, RA/CTS HMW induced the highest level of serum anti-OVA IgG antibodies (Figure 11B). Based on these results, RA/CTS HMW was selected as the formulation for all further in vivo experiments.

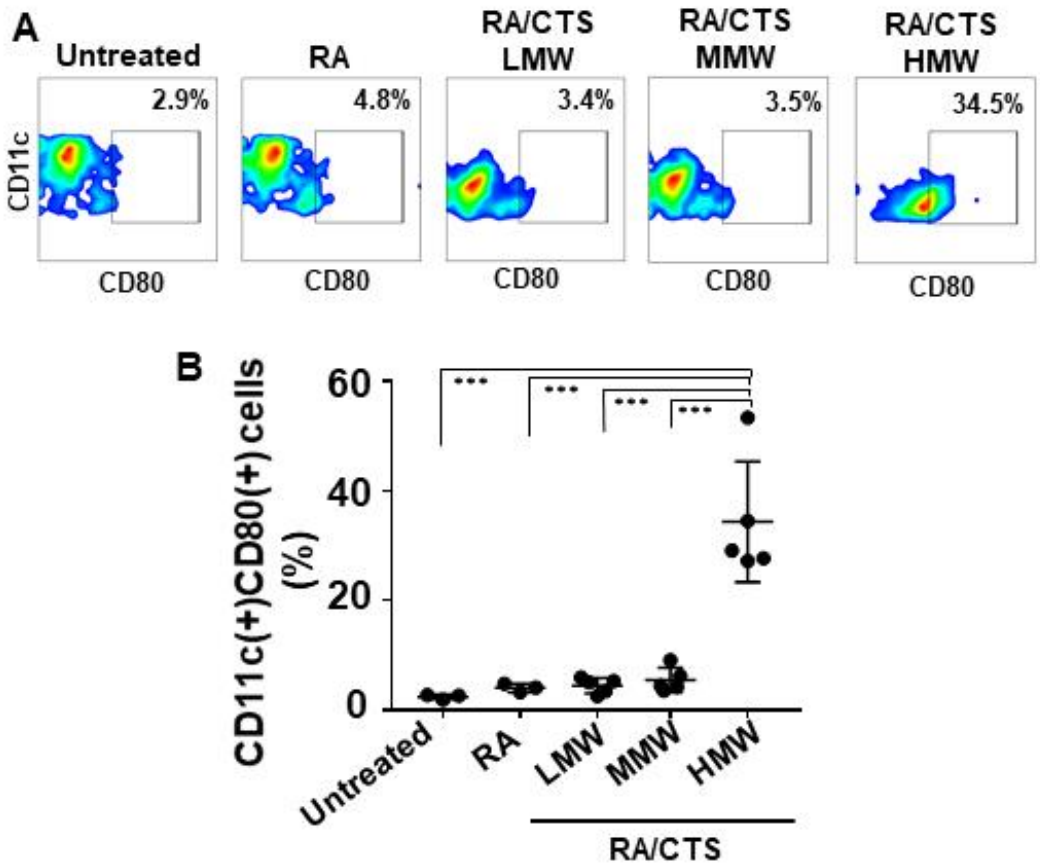

Figure 10. Adjuvant effect of RA/CTS dependent on molecular weight of CTS.

Splenic dendritic cells were treated with various formulations of RA/CTS. After 24 hours, the surface expression of CD80 on DCs was measured (A) and analyzed (B) by flow cytometry (***$P < 0.005$).

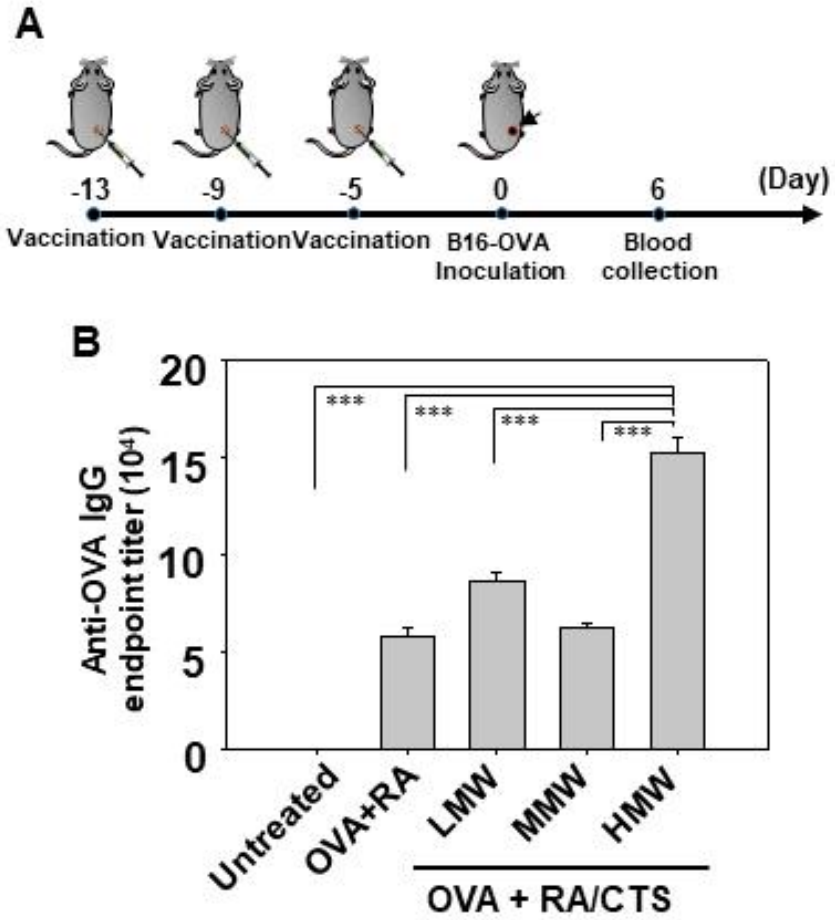

Figure 11. Immune boosting effect of various RA/CTS nanocomplexes.

Naive C57BL/6 mice were vaccinated with RA/CTS physically mixed with OVA antigen (100 μg) every 4 days for 3 times. Five days after the last vaccination (day 0), mice were inoculated with B16-OVA cells (s.c.) (A). Six days after inoculation, blood samples were collected for serum anti-OVA IgG titration at different dilution factors (B). Data shown as mean ± SEM, n = 4. ***$P < 0.005$.

3.7 *In vivo* DC maturation by RA/CTS

DC maturation was tested with splenocytes isolated from mice after treatment with RA/CTS HMW for 24 hours (Figure 12A). The RA/CTS-treated group showed significantly higher expression of both CD80 and CD86 markers than other control groups (Figure 12B). The CD80 (Figure 12C) or CD86 (Figure 12D)-positive populations of RA/CTS-treated group were 74.8 ± 6.6% or 52.2 ± 8.77%, respectively.

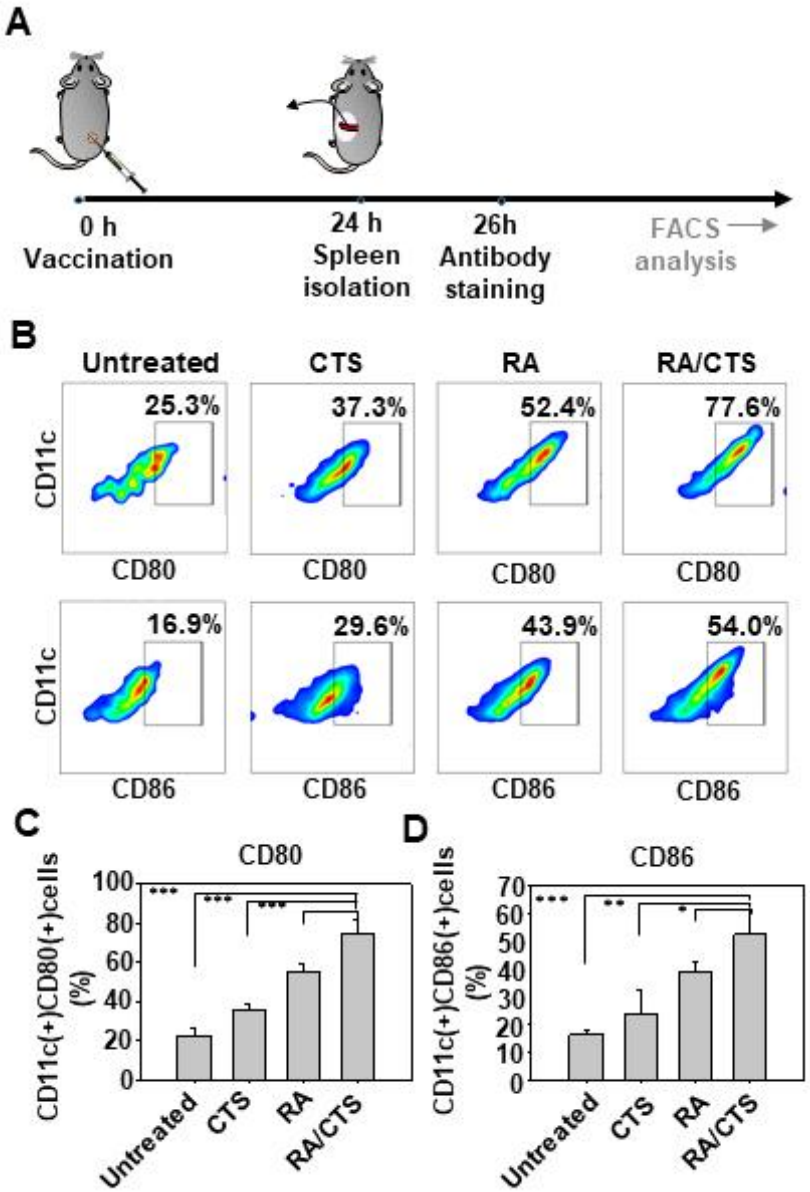

Figure 12. *In vivo* DC maturation effect of RA/CTS.

Naive C57BL/6 mice were administered with RA/CTS HMW at 10 μg RA dose. After 24 hours, splenocytes from those mice were isolated to measure surface expression of CD80 and CD86 on CD11c+cells by flow cytometry (A). CD80 (B) or CD86 (C) expressing DC populations for each group were quantified (*P < 0.05; **P <0.01; ***P <0.005).

3.8 *In vivo* antitumor efficacy

Tumor prevention effect of RA/CTS was demonstrated with B16-OVA tumor-bearing mice. The RA/CTS and OVA as a model antigen were given every 4 days before tumor inoculation (Figure 13A). Immunized mice were challenged with B16-OVA cells five days after last vaccination. In the OVA + RA treated group, 40% (4/10) of mice showed tumorigenesis while 100% of untreated or OVA-treated mice failed to prevent tumor growth (Figure 13B). In contrast, OVA + RA/CTS-treated group showed 80% (8/10) of complete regression without tumor development. In addition, on the last day (day 33) of monitoring period for mice, the biggest tumor volume of OVA + RA/CTS-treated group was 204mm^3 while those of untreated, OVA, and OVA + RA-treated groups were 2246mm^3, 6491mm^3, and 1507mm^3, respectively. The highest survival rate was observed with OVA + RA/CTS-treated group (Figure 14B).

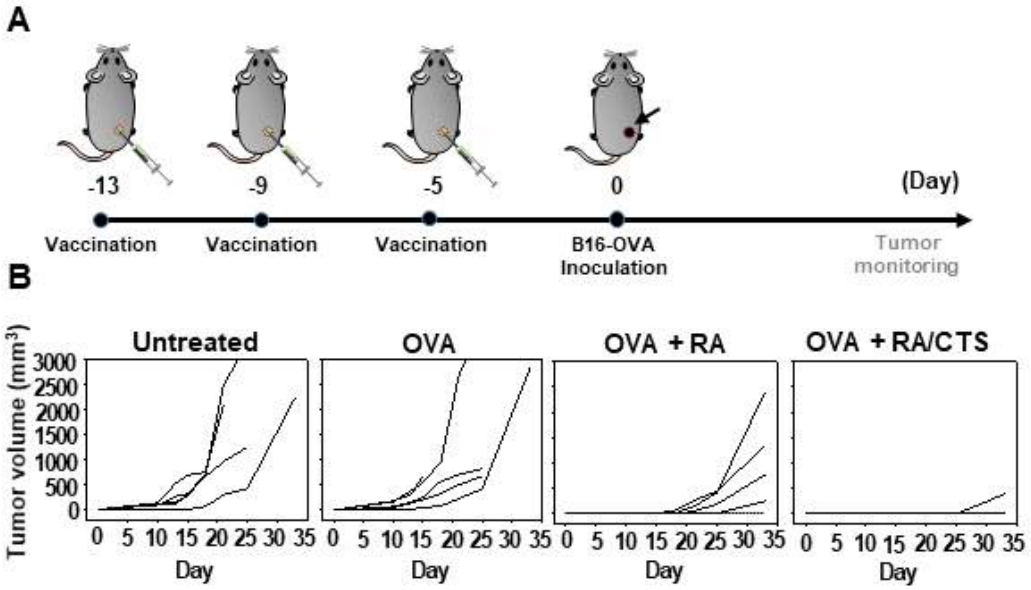

Figure 13. *In vivo* antitumor effects of RA/CTS post-vaccination. Timeline for in vivo experiments was indicated (A). Naive C57BL/6 mice were vaccinated with RA/CTS physically mixed with OVA antigen (100 μg) every 4 days (day -13, -9, -5) for 3 times. Five days after the last vaccination (day 0), mice were inoculated with B16-OVA cells ($3x10^5$) subcutaneously. Tumor volumes were measured regularly until day 33 after tumor inoculation (B).

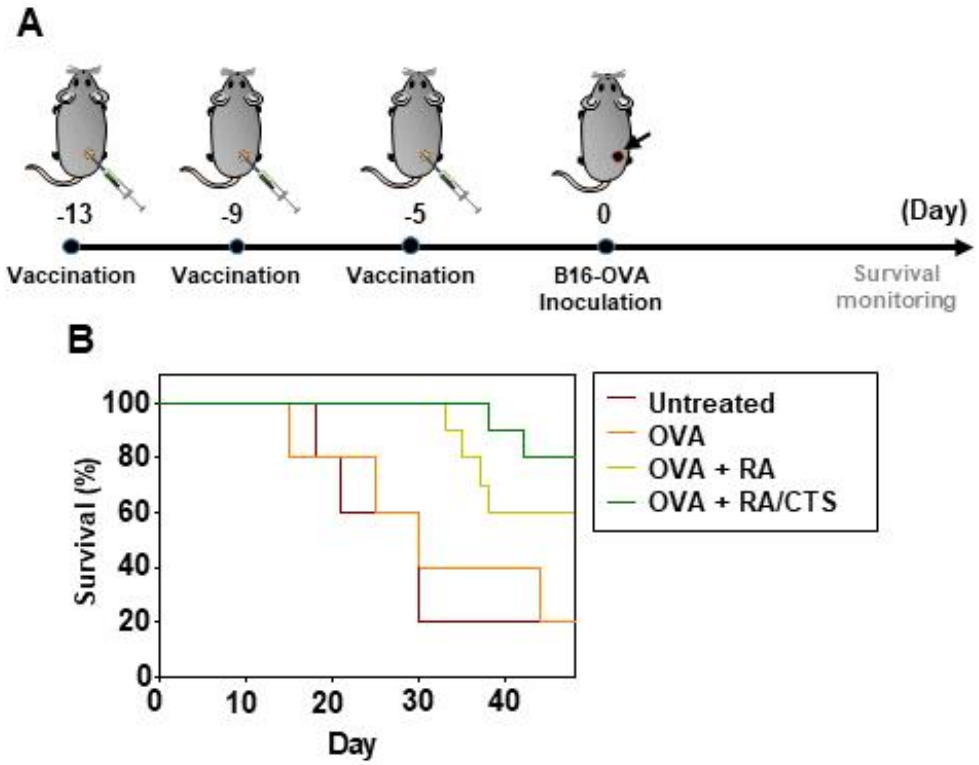

Figure 14. Survival rates after vaccination with RA/CTS.

Timeline for in vivo experiments was indicated (A). Survival rates of mice were monitored until day 48 (B).

3.9 *In vivo* cellular immune response of RA/CTS vaccination

To explore mechanisms underlying antitumor efficacy of RA/CTS, cellular immune response was examined after tumor challenge. Cellular immune response was evaluated by functionality of splenocytes isolated from immunized mice 2 days after the tumor challenge (Figure 15A). IFN-γ producing CD8+ T cells from immunized mice were detected upon re-stimulation with OVA peptide (Figure 15B, 15C). The OVA + RA/CTS-treated splenocytes showed the highest number of IFN-γ-secreting cells compared to the control groups (Figure 15B). There were 14.5 times more IFN-γ-secreting cells in OVA + RA/CTS-treated group than in OVA treated group (Figure 15C).

On day 27 after tumor challenge, tumor infiltration of CD4+ and CD8+ T cells were evaluated by flow cytometry (Figure 16A). Highest percentage of CD4+ (Figure 16B) and CD8+ T cells (Figure 16C) infiltrated the tumor tissues in OVA + RA/CTS-treated mice.

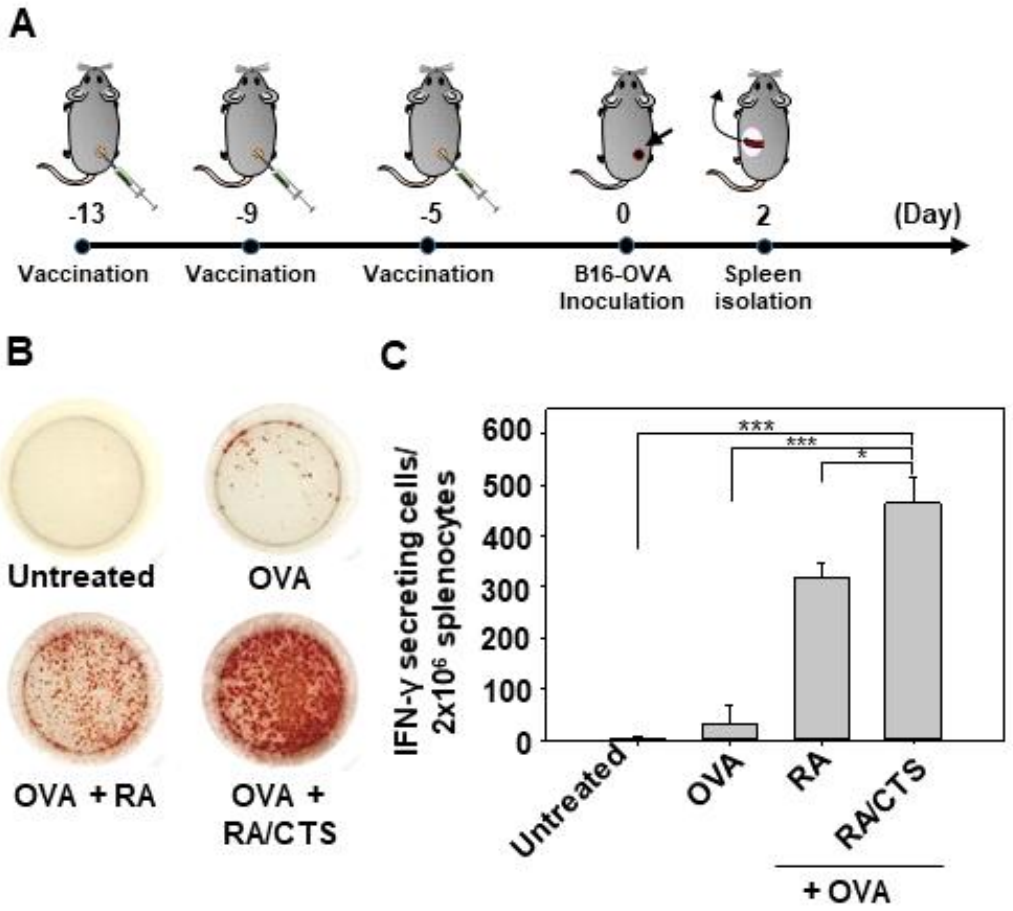

Figure 15. Cellular immune responses post-vaccination.

Naive C57BL/6 mice were vaccinated with RA/CTS physically mixed with OVA antigen every 4 days for 3 times. Five days after the last vaccination (day 0), mice were inoculated with B16-OVA cells ($3x10^5$) (A). After 2 days, splenocytes were isolated for ex-vivo IFN-γ ELISPOT (B). IFN-γ secreting cells per $2x10^7$ splenocytes were counted using stereomicroscope (C) (*P <0.05; ***P <0.005).

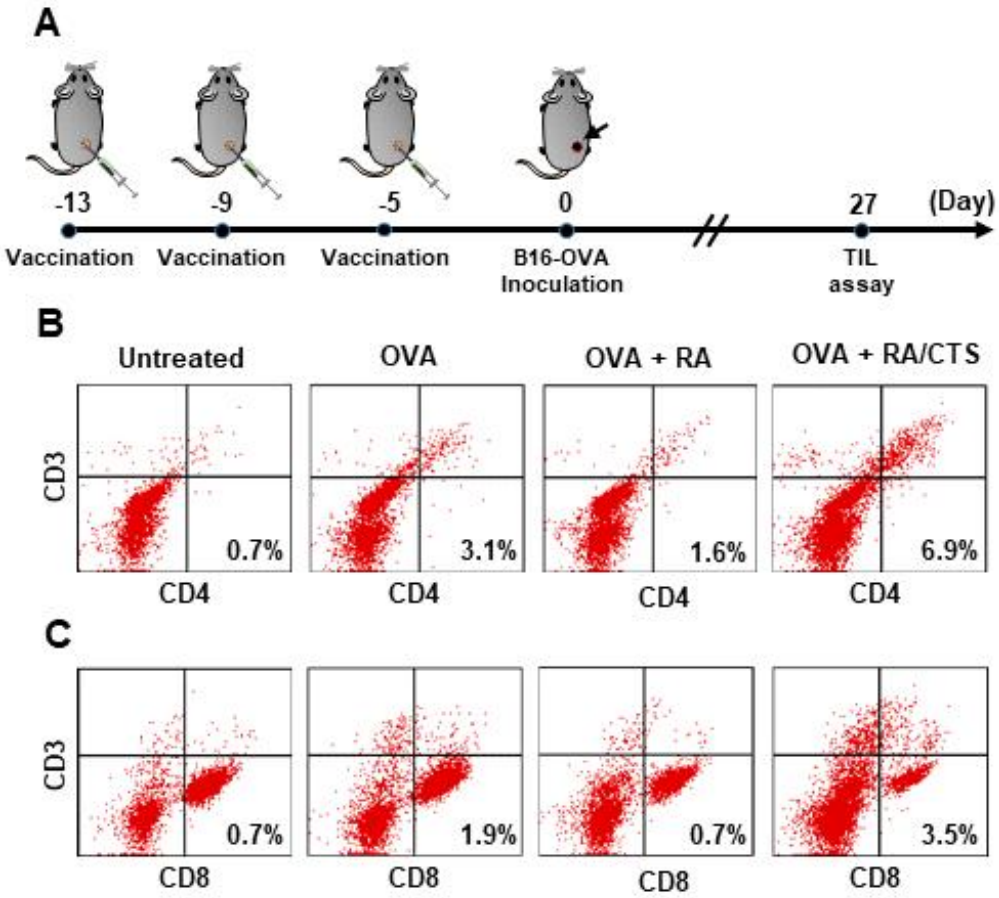

Figure 16. Tumor infiltrating T cells post-vaccination.

Timeline for this assay is indicated (A). Tumor-infiltrating T cells in tumors were analyzed for CD3+CD4+ T helper cells (B) and CD3+CD8+ cytotoxic T cells (C) by flow cytometry on day 27.

3.10 *In vivo* humoral immune response of RA/CTS vaccination

For antigen-specific humoral immune response, serum anti-OVA IgG levels were measured by ELISA at two time points (Figure 17A). On day 6 and 10 after tumor inoculation, OVA + RA/CTS-treated mice showed much higher anti-OVA titer against OVA antigen compared to the other groups (Figure 17B, 17C).

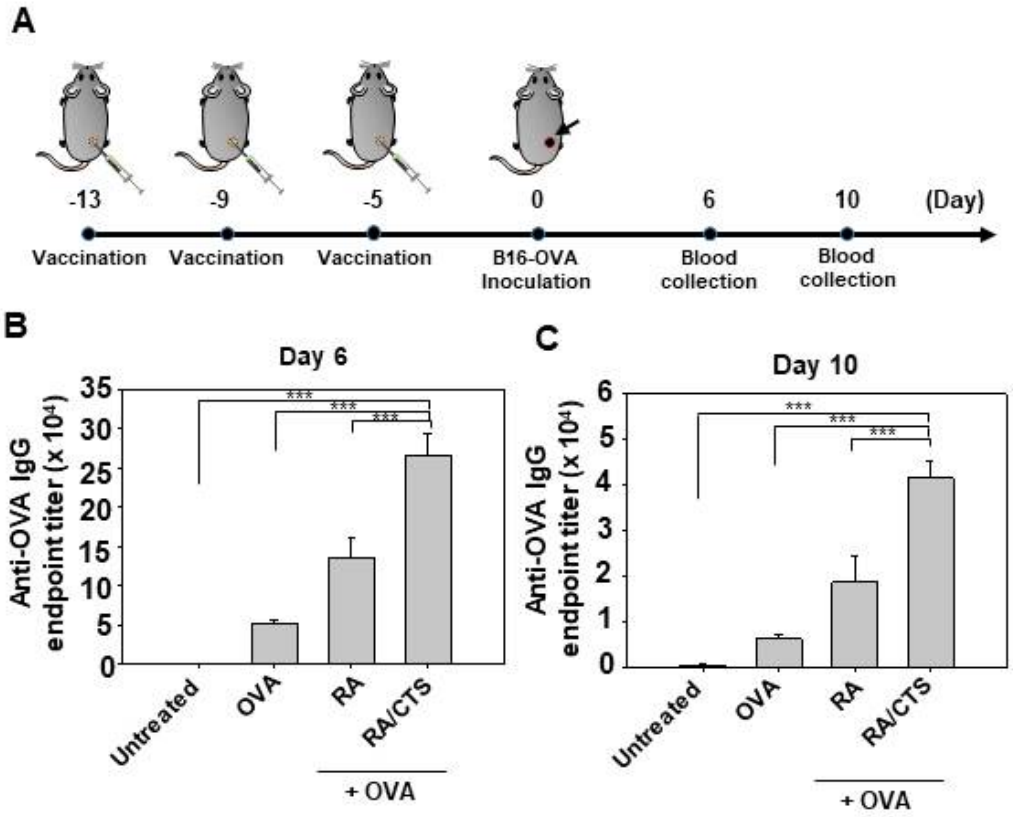

Figure 17. Humoral response post-vaccination.

Blood samples were collected for serum anti-OVA IgG titration 6 and 10 days after inoculation (A). Serum anti-OVA IgG levels were measured by ELISA (***$P < 0.005$) (B-C).

3.11 Antitumor effect against secondarily challenged tumor

Protection of tumor recurrence was evaluated by re-challenging the immunized mice 69 days after the first tumor challenge with approximately 6 times more tumor cells (Figure 18A). Mice were not re-vaccinated before the re-challenge. The OVA + RA/CTS-treated mice were not fully protected from tumor recurrence but compared to control groups, tumor growth was substantially delayed (Figure 18B). On the last day of monitoring tumor volume, the average volume of OVA + RA/CTS-treated group was 480.0 ± 442.2 mm^3 while untreated and OVA + RA-treated groups were 7318 ± 3598.7 mm^3, and 3674.8 ± 212.5 mm^3, respectively. Survival rates were also monitored during this period (Figure 19A). The rates clearly differed among the groups with only the OVA + RA/CTS-treated mice surviving 100% by the 40th day after tumor re-challenge (Figure 19B). For untreated and OVA + RA-treated mice, only 33% were surviving by the 40th day.

3.12 Long-term protection of tumor recurrence

To demonstrate the mechanism behind long-term protection from tumor recurrence, memory effector T cells (CD3+CD8+ $CD44^{high}CD62L^{low}$) in inguinal lymph nodes were analyzed 9 days after tumor re-challenge (Figure 20A). Flow cytometry results revealed the highest percentage of memory effector T cells for OVA + RA/CTS-treated mice (Figure 20B, 20C). Untreated group showed the lowest percentage of memory effector T cells

(12.1 ± 1.65 %), whereas the OVA +RA/CTS-treated group of 18.9 ± 1.02 %, corresponding with the lowest tumor volume during the monitoring (Figure 20B, 20C).

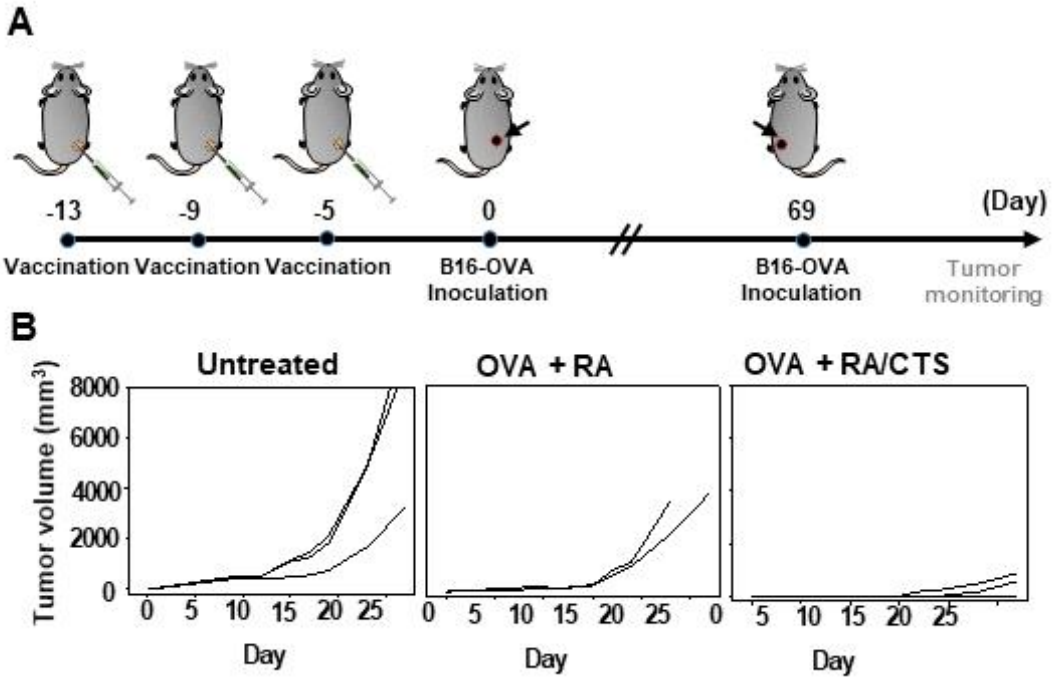

Figure 18. Antitumor effect after tumor re-challenge.

Naive mice were vaccinated with RA/CTS HMW physically mixed with OVA antigen every 4 days for 3 times. Five days after the last vaccination (day 0), mice were inoculated with B16-OVA cells ($3x10^5$). At 69 days after inoculation, mice were re-inoculated with B16-OVA cells ($2x10^6$) (A) and tumor sizes were measured for 27 days (B).

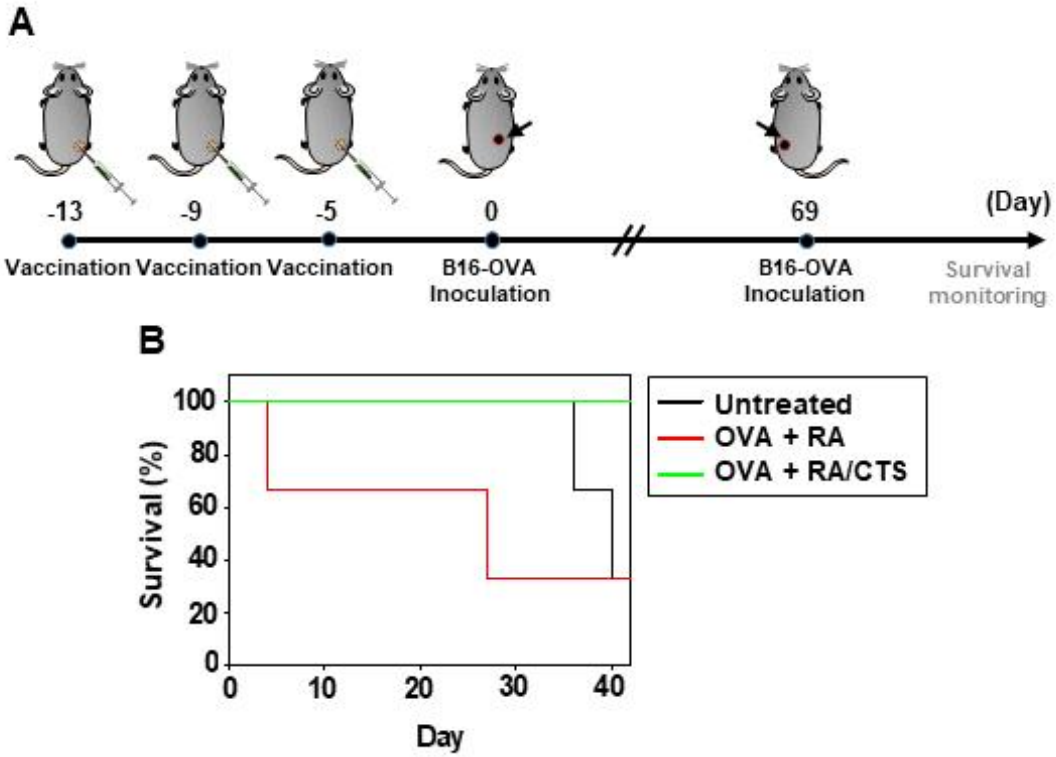

Figure 19. Survival rates after tumor re-challenge.

Vaccinated mice were re-challenged with B16-OVA cells ($2x10^6$) 69 days after the first inoculation. Survival rates were monitored for 42 days from the re-challenge.

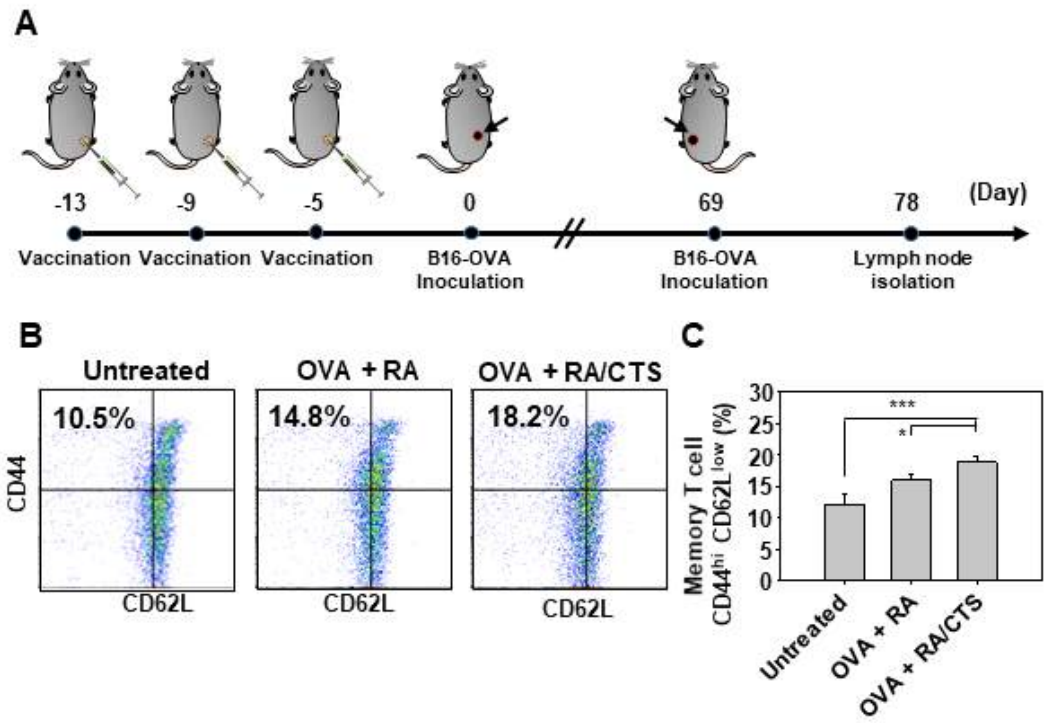

Figure 20. Mechanism for long-term protection of tumor recurrence.

Tumor-draining lymph nodes were analyzed for effector memory T cells 9 days after the tumor re-challenge (A). The percentage of effector memory T cells ($CD3+CD8+CD44^{high}CD62L^{low}$) for each group was quantified ($*P < 0.05$; $***P < 0.005$) (B-C).

4. Discussion

In this study, we demonstrated that RA/CTS served as a remarkable nano-vaccine for cancer treatment. RA/CTS successfully generated humoral and cellular immune responses against model tumor antigen, and exerted long-term prevention of tumorigenesis.

The RA is condensed into a nanocomplex due to the electrostatic charge interaction with CTS. The characterization of RA/CTS nanocomplex was well defined in the range of sub-micron size (Figure 4A, 4B) with a positive surface charge (Figure 5). The sub-micron size of adjuvant complex is necessary for the high chance of phagocytosis by antigen presenting cells compared to RA alone [17]. The main cellular uptake pathways of RA/CTS nanocomplexes would be clathrin-mediated endocytosis and macropinocytosis (Figure 8). We observed that the cellular uptake of RA/CTS was significantly decreased upon the inhibition of clathrin-mediated endocytosis by chlorpromazine/sucrose, and macropinocytosis by amiloride. Similar to our observation, it has been reported that CTS-based nanoparticles were internalized to the cells by clathrin-mediated pathway and macropinocytosis [18].

At the optimized RA/CTS complexation ratio of 1:10, the surface of nanocomplexes had a net positive charge. OVA protein, a well-known model antigen, carries a negative charge at pH 7, ranging from -1 to -27mV [18-19]. Therefore, positive charge of RA/CTS nanocomplexes may support the adsorption of

the antigens, which is necessary to produce the antigen–adjuvant complex for an efficient immune trigger. Because most human antigens are known to possess negative charge [20–21], our RA/CTS nanocomplexes will not only be effective with OVA but could potentially interact with other tumor antigens as well.

By combining RNA adjuvant with CTS, we have generated a stable nanocomplex in serum conditions or under presence of RNase (Figure 7). One of the biggest challenges of using RNA adjuvant is the fast degradation in physiological conditions. RNA could be degraded within several minutes in body fluid due to the digestion of endonuclease [22]. This stability issue can be bypassed by chemically modifying RNA. These modifications, such as modifying ribose rings of the nucleotide or inserting nuclease resistant linkages [23], however, raise issues for large scale production and toxicities [23–25]. Indeed, chemical modification requires multistep optimization and screening to guarantee similar efficacy. Complexation with CTS, however, mainly generates a cover backbone providing steric hindrance, thus preventing the attack of nucleases [26]. Therefore, CTS would provide the protection that RA needs while maintaining the inherent structure of RNA as well as the pharmacodynamics and safety profile of this material.

The RA/CTS nanocomplexes showed the best immunostimulatory effect when formed with high molecular weight CTS. Although additional studies may be required to explain this phenomenon, it has been reported that the higher the molecular weight of CTS the stronger the ability to intertwine with RA due to its highly positive charge [27].

Indeed, high molecular weight CTS has shown much better protection of nucleic acids against in vivo conditions including serum proteins and enzymes. Our study has revealed that high molecular weight CTS induced stronger immune response than lower molecular weights. It could be explained by the stable complexation and efficient protection from serum degradation of higher molecular weight CTS.

RA, a defined molecular weight-derivative of poly I:C, will behave as a toll-like receptor (TLR) 3 agonist. Poly I:C, a synthetic double stranded RNA, is known to be agonists of TLR3. TLR3-mediated toll/interleukin-1 receptor domain-containing adaptor-inducing interferon-B (TRIF) pathway leads to production of pro-inflammatory cytokines like IL-6, chemokines, and most importantly, maturation of dendritic cells [28]. Although poly I:C is a very effective adjuvant, the clinical translation of poly I:C for human use still remains limited due to undefined structure and poor homogeneity [29]. Indeed, poly I:C activity is molecular weight-dependent and has shown inconsistent activities depending on vendors [30]. RA/CTS nanocomplex is hypothesized to overcome the molecular weight variation issue of poly I:C for human use.

Subcutaneous route was chosen for RA/CTS vaccination. Systemic administration of nucleic acid adjuvant can induce massive cytokine storm that results in systemic side effects [5]. Therefore, local injections such as intradermal or subcutaneous routes may be the preferred routes for RA/CTS. Moreover, most clinically accepted routes for vaccination are via intramuscular or subcutaneous routes due to relatively easy access, potential for

consistent delivery, and sufficient immunogenicity [31]. Only a limited amount of antigens can be detected in muscle-draining lymph nodes with traditional vaccines delivered via intramuscular route [32-33]. Subcutaneous route, on the other hand, provides efficient lymphatic drainage which could increase vaccine delivery to nearby draining lymph nodes [33-34].

The primary goal of cancer vaccination is to prime tumor antigen-specific T cells to recognize and eliminate tumor cells. RA, by TLR3-mediated activation, maturates DCs and enhances cross-presentation of the antigens by upregulating MHC-I, CD80/86 expression on DCs [17]. This enhanced antigen presentation activates naive CD8+ T cells as well as CD4+ T cells. CD8+ cytotoxic T cell generation is critical for antitumor activity and DCs are one of the most potent cross-presenting APC in vivo [4]. CTS nanoparticles are thought to enhance cellular and humoral immune response [35-36] possibly through DC maturation [37]. By incorporating OVA protein as model antigen, we confirmed OVA-specific humoral and cellular immune response (Figure 8). Highest number of IFN-γ producing T cells in RA/CTS group illustrated successful cross-antigen presentation and cytotoxic T cell priming.

In order to evaluate RA/CTS nanocomplex as a prophylactic cancer vaccine, B16-OVA was chosen as the tumor model. Melanoma is known as an aggressive tumor with high risk of recurrence and metastasis. Here, we examined the protection efficacy of vaccinated mice by challenging with B16-OVA tumor. The suppression of tumor was clearly observed. Consistent with high antibody levels as well as antigen-specific CD8+ T cells,

higher number of both CD4+ and CD8+ tumor infiltrating lymphocytes were observed. These results serve as clear evidence for antitumor response generated by RA/CTS vaccination. Long term prevention of tumor is also a critical purpose of cancer vaccine. By re-challenging with same tumor cells, long term protection was observed by considerable delay in tumor growth. Our vaccination provided antitumor which protect mice form tumor growth after a long-term. This could be explained by higher percentage of memory effector T cells in the RA/CTS-treated mice re-challenged with tumor [13, 38].

5. Conclusion

In this study, we provided evidence that RA/CTS nanocomplexes could serve as an effective nanoadjuvant of tumor antigens. Through complexation with CTS, the TLR3-type adjuvant effect of RA was significantly enhanced. Although we used OVA as a model tumor antigen, RA/CTS nanocomplex could be combined with other tumor antigens to induce immune responses that prevent the uncontrolled growth of tumors expressing different specific antigens.

6. References

1. Finn, O.J. The dawn of vaccines for cancer prevention. *Nat. Rev. Immunol.* 2018, *18*, 183.

2. Temizoz, B.; Kuroda, E.; Ishii, K.J. Vaccine adjuvants as potential cancer immunotherapeutics. *Int. Immunol.* 2016, *28*, 329-338.

3. HogenEsch, H. Mechanism of immunopotentiation and safety of aluminum adjuvants. *Front. Immunol.* 2013, *3*, 406.

4. Ammi, R.; De Waele, J.; Willemen, Y.; Van Brussel, I.; Schrijvers, D.M.; Lion, E.; Smits, E.L. Poly (I: C) as cancer vaccine adjuvant: knocking on the door of medical breakthroughs. *Pharmacol. Ther.* 2015, *146*, 120-131.

5. Ziegler, A.; Soldner, C.; Lienenklaus, S.; Spanier, J.; Trittel, S.; Riese, P.; Kramps, T.; Weiss, S.; Heidenreich, R.; Jasny, E. A new RNA-based adjuvant enhances virus-specific vaccine responses by locally triggering TLR-and RLH-dependent effects. *J. Immunol.* 2017, *198*, 1595-1605.

6. Shirota, H.; Tross, D.; Klinman, D.M. CpG oligonucleotides as cancer vaccine adjuvants. *Vaccines* 2015, *3*, 390-407.

7. Adamus, T.; Kortylewski, M. The revival of CpG oligonucleotide-based cancer immunotherapies. *Contemp. Oncol.* 2018, *22*, 56-60, doi:10.5114/wo.2018.73887.

8. Wang, R.; Miyahara, Y.; Wang, H. Toll-like receptors and immune regulation: implications for cancer therapy. *Oncogene* 2008, *27*, 181.

9. Frank-Bertoncelj, M.; Pisetsky, D.S.; Kolling, C.; Michel, B.A.; Gay, R.E.; J□ngel, A.; Gay, S. TLR3 ligand poly (I: C) exerts distinct actions in synovial fibroblasts when delivered by extracellular vesicles. *Front. Immunol.* 2018, *9*, 28.

10. Cao, Y.; Tan, Y.F.; Wong, Y.S.; Liew, M.W.J.; Venkatraman, S. Recent Advances in Chitosan-Based Carriers for Gene Delivery. *Mar. drugs* 2019, *17*, 381.

11. Zhang, H.; Chen, S.; Zhi, C.; Yamazaki, T.; Hanagata, N. Chitosan-coated boron nitride nanospheres enhance delivery of CpG oligodeoxynucleotides and induction of cytokines. *Int. J. Nanomed.* 2013, *8*, 1783.

12. Alameh, M.; Lavertu, M.; Tran-Khanh, N.; Chang, C.Y.; Lesage, F.; Bail, M.; Darras, V.; Chevrier, A.; Buschmann, M.D. siRNA Delivery with Chitosan: Influence of Chitosan Molecular Weight, Degree of Deacetylation, and Amine to Phosphate Ratio on in Vitro Silencing Efficiency, Hemocompatibility, Biodistribution, and in Vivo Efficacy. *Biomacromolecules* 2018, *19*, 112-131, doi:10.1021/acs.biomac.7b01297.

13. Le, Q.-V.; Suh, J.; Choi, J.J.; Park, G.T.; Lee, J.W.; Shim, G.; Oh, Y.-K. In Situ Nanoadjuvant-Assembled Tumor Vaccine for Preventing Long-Term Recurrence. *ACS Nano* 2019, *13*, 7442-7462.

14. Nabi, I.R.; Le, P.U. Caveolae/raft-dependent endocytosis. *J Cell Biol.* 2003, *161*, 673-677.

15. Dutta, D.; Donaldson, J.G. Search for inhibitors of endocytosis: Intended specificity and unintended consequences. *Cell Logist.* 2012, *2*, 203-208.

16. Van Nguyen, T.; Shin, M.C.; Min, K.A.; Huang, Y.; Oh, E.; Moon, C. Cell-penetrating peptide-based non-invasive topical delivery systems. *J. Pharm. Investig.* 2018, *48*, 77-87.

17. Wculek, S.K.; Cueto, F.J.; Mujal, A.M.; Melero, I.; Krummel, M.F.; Sancho, D. Dendritic cells in cancer immunology and immunotherapy. *Nat. Rev. Immunol.* 2019, 1-18.

18. Mou, Y.; Xing, Y.; Ren, H.; Cui, Z.; Zhang, Y.; Yu, G.; Urba, W.J.; Hu, Q.; Hu, H. The effect of superparamagnetic iron oxide nanoparticle surface charge on antigen cross-presentation. *Nanoscale Res. Lett.* 2017, *12*, 52.

19. Dombu, C.; Carpentier, R.; Betbeder, D. Influence of surface charge and inner composition of nanoparticles on intracellular delivery of proteins in airway epithelial cells. *Biomaterials* 2012, *33*, 9117-9126.

20. Henriksen-Lacey, M.; Christensen, D.; Bramwell, V.W.; Lindenstrøm, T.; Agger, E.M.; Andersen, P.; Perrie, Y. Liposomal cationic charge and antigen adsorption are important properties for the efficient deposition of antigen at the injection site and ability of the vaccine to induce a CMI response. *J. Control. Release* 2010, *145*, 102-108.

21. Wang, M.; Zhu, D.; Zhu, J.; Nussinov, R.; Ma, B. Local and global anatomy of antibody-protein antigen recognition. *J. Mol. Recognit.* 2018, *31*, e2693.

22. Singh, A.; Trivedi, P.; Jain, N.K. Advances in siRNA delivery in cancer therapy. *Artif. Cell Nanomed. B.* 2018, *46*, 274-283.

23. Corey, D.R. Chemical modification: the key to clinical application of

RNA interference? *J. Clin. Investig.* 2007, *117*, 3615-3622.

24. Swayze, E.E.; Siwkowski, A.M.; Wancewicz, E.V.; Migawa, M.T.; Wyrzykiewicz, T.K.; Hung, G.; Monia, B.P.; Bennett; Frank, C. Antisense oligonucleotides containing locked nucleic acid improve potency but cause significant hepatotoxicity in animals. *Nucleic Acids Res.* 2006, *35*, 687-700.

25. Kakiuchi-Kiyota, S.; Koza-Taylor, P.H.; Mantena, S.R.; Nelms, L.F.; Enayetallah, A.E.; Hollingshead, B.D.; Burdick, A.D.; Reed, L.A.; Warneke, J.A.; Whiteley, L.O. Comparison of hepatic transcription profiles of locked ribonucleic acid antisense oligonucleotides: evidence of distinct pathways contributing to non-target mediated toxicity in mice. *Toxicol. Sci.* 2013, *138*, 234-248.

26. Speth, M.T.; Repnik, U.; Müller, E.; Spanier, J.; Kalinke, U.; Corthay, A.; Griffiths, G. Poly (I: C)-encapsulating nanoparticles enhance innate immune responses to the tuberculosis vaccine Bacille Calmette-Gu□rin (BCG) via synergistic activation of innate immune receptors. *Mol. Pharm.* 2017, *14*, 4098-4112.

27. Akbuga, J.; Ozbas-Turan, S.; Ekentok, C. Chitosan Nanoparticles in Gene Delivery. In *Percutaneous Penetration Enhancers Chemical Methods in Penetration Enhancement*, Springer: 2016; pp. 337-351.

28. Kreutz, M.; Bakdash, G.; Dolen, Y.; Sk□ld, A.E.; van Hout-Kuijer, M.A.; de Vries, I.J.M.; Figdor, C.G. Type I IFN-mediated synergistic activation of mouse and human DC subsets by TLR agonists. *Eur. J. Immunol.* 2015, *45*, 2798-2809, doi:10.1002/eji.201545583.

29. Naumann, K.; Wehner, R.; Schwarze, A.; Petzold, C.; Schmitz, M.; Rohayem, J. Activation of dendritic cells by the novel Toll-like

receptor 3 agonist RGC100. *Clin. Dev. Immunol.* 2013, *2013*.

30. Mian, M.F.; Ahmed, A.N.; Rad, M.; Babaian, A.; Bowdish, D.; Ashkar, A.A. Length of dsRNA (poly I: C) drives distinct innate immune responses, depending on the cell type. *J. Leukoc. Biol.* 2013, *94*, 1025-1036.

31. Singh, B.; Maharjan, S.; Sindurakar, P.; Cho, K.-H.; Choi, Y.-J.; Cho, C.-S. Needle-free immunization with chitosan-based systems. *Int. J. Mol. Sci.* 2018, *19*, 3639.

32. Dupuis, M.; McDonald, D.M.; Ott, G. Distribution of adjuvant MF59 and antigen gD2 after intramuscular injection in mice. *Vaccine* 1999, *18*, 434-439.

33. Kuai, R.; Sun, X.; Yuan, W.; Xu, Y.; Schwendeman, A.; Moon, J.J. Subcutaneous nanodisc vaccination with neoantigens for combination cancer immunotherapy. *Bioconjug. Chem.* 2018, *29*, 771-775.

34. Moyer, T.J.; Zmolek, A.C.; Irvine, D.J. Beyond antigens and adjuvants: formulating future vaccines. *J. Clin. Invest.* 2016, *126*, 799-808.

35. Malik, A.; Gupta, M.; Gupta, V.; Gogoi, H.; Bhatnagar, R. Novel application of trimethyl chitosan as an adjuvant in vaccine delivery. *Int. J. Nanomed.* 2018, *13*, 7959.

36. Liu, Q.; Zheng, X.; Zhang, C.; Shao, X.; Zhang, X.; Zhang, Q.; Jiang, X. Conjugating influenza a (H1N1) antigen to n-trimethylaminoethylmethacrylate chitosan nanoparticles improves the immunogenicity of the antigen after nasal administration. *J. Med. Virol.* 2015, *87*, 1807-1815.

37. Carroll, E.C.; Jin, L.; Mori, A.; Muñoz-Wolf, N.; Oleszycka, E.; Moran, H.B.; Mansouri, S.; McEntee, C.P.; Lambe, E.; Agger, E.M. The vaccine adjuvant chitosan promotes cellular immunity via DNA sensor cGAS-STING-dependent induction of type I interferons. *Immunity* **2016**, *44*, 597-608.

38. Chen, Q.; Xu, L.; Liang, C.; Wang, C.; Peng, R.; Liu, Z. Photothermal therapy with immune-adjuvant nanoparticles together with checkpoint blockade for effective cancer immunotherapy. *Nat. Commun.* **2016**, *7*, 13193.

국문초록

핵산 어쥬번트는 면역세포가 암세포를 억제하도록 유도하기 위한 암 백신의 한 종류로서 최근 활발하게 연구되고 있다. 본 연구에서는 핵산 어쥬번트와 키토산의 복합체를 설계하여 면역 증강 효과를 확인하였다. Toll-like receptor 3을 인지하는 RNA 핵산 어쥬번트 (RA)는 음전하를 띄고 있으며 양이온성 고분자 키토산과 결합하여 양전하 제타전위를 가진 나노복합체(RA/CTS)를 형성하였다. 이 RA/CTS 복합체는 수지상세포에 처리하였을 때 특별한 독성 없이 수지상세포 성숙화를 유도하였는데 특히 여러 가지의 키토산 분자량 중 340 kDa 키토산이 RA와 결합하였을 때 효과가 가장 높았다. 340 kDa 키토산을 이용한 RA/CTS 복합체와 모델 항원 ovalbumin (OVA)을 쥐에 3회 피하주사하고 OVA항원을 발현하는 종양을 유도하였을 때 종양의 형성이 억제되는 효과를 관찰하였다. 또한, 면역화 된 쥐에 2차로 종양을 유도하였을 때 RA/CTS 처리군이 가장 큰 종양 억제효과를 보였다. 이러한 항종양 효과는 암 항원 특이적 체액성 면역반응과 세포성면역 반응, 그리고 종양조직 내 CD4와 CD8 T세포의 유입에 의한 것으로 판단된다. OVA와 RA/CTS 복합체를 주사한 쥐들은 2차 암 유도 후에도 가장 높은 생존율을 보였다. 이러한 결과들은 RA/CTS 복합체가 효과적인 나노어쥬번트로서 암 백신과 면역치료에 유용하게 쓰일 수 있음을 보여준다.

주요어 : RNA 어쥬번트, 키토산, 나노어쥬번트, 암 백신, 면역치료
학 번 : 2017-27650